A method for determining the position of FBG sensors accurately

Rajabzadeh, Aydin; Hendriks, Richard C.; Heusdens, Richard; Groves, Roger M.

DOI
10.1117/12.2545756

Publication date
2019

Document Version
Final published version

Published in
Seventh European Workshop on Optical Fibre Sensors

A method for determining the position of FBG sensors accurately

Aydin Rajabzadeh, Richard C. Hendriks, Richard Heusdens, Roger M. Groves

Aydin Rajabzadeh, Richard C. Hendriks, Richard Heusdens, Roger M. Groves, "A method for determining the position of FBG sensors accurately," Proc. SPIE 11199, Seventh European Workshop on Optical Fibre Sensors, 111990U (28 August 2019); doi: 10.1117/12.2545756

SPIE.

Event: Seventh European Workshop on Optical Fibre Sensors, 2019, Limassol, Cyprus

A Method for Determining the Position of FBG Sensors Accurately

Aydin Rajabzadeh[a,b], Richard C. Hendriks[a], Richard Heusdens[a], and Roger M. Groves[b]

[a] Circuits and Systems group, Delft University of Technology, Delft, 2628 CD, The Netherlands
[b] Structural Integrity and Composites group, Faculty of Aerospace Engineering, Delft University of Technology, Delft, 2629 HS, The Netherlands

ABSTRACT

Fibre Bragg grating sensors have gained a lot of attention in damage detection and strain measurement applications in the past few decades. These applications include matrix crack detection and delamination tip monitoring in composite structures, crack detection in concrete and civil engineering structures and etc. The damage localisation accuracy of such methods, directly depends on precise knowledge on the position of the FBG sensor. However, this information is not commonly provided by manufacturing companies with such accuracy. In this paper, we propose a novel approach to accurately determine the position of an FBG sensor with a low complexity setup. The proposed method offers an accuracy of below $10\,\mu m$, and can consequently increase the spatial resolution of damage detection methods.

Keywords: Accuracy, FBG, Fibre Bragg grating, Fibre optic sensors, Structural health monitoring

1. INTRODUCTION

Fibre Bragg grating (FBG) sensors are typically used in point strain and temperature measurement applications.[1,2] In recent years, the application of FBG sensors in damage detection of a variety of materials and structures has gained a lot of attention as well.[3–5] Due to the small diameter and low weight of these sensors, they can be embedded between the layers of composite structures, and provide useful information about the structural integrity of the internal layers of the composite material.[6]

In all the above mentioned applications, it is essential to know the precise position of the FBG sensor along the optical fibre, so that it provides useful data for engineering models of structural integrity. For instance, using the FBG sensors in the detection of barely visible matrix cracks in composites,[3,5] or monitoring the growth and progress of delaminated composite layers, the knowledge of the precise location of the cracks or the delamination tip[4] can be very useful in studying the fatigue and stress behaviour of composites. The accuracy of damage localisation and progression in these applications directly depends on having a precise knowledge of the exact position of the FBG sensor. However, when the FBG is received from the manufacturer, there is usually ambiguity in the exact position of the FBG, as the sensor markings only indicate the approximate position of the sensor. For some manufacturing methods (e.g. strip and recoat method), it is possible to achieve higher accuracies using more precise translation stages, but the production costs increase significantly.

In this paper, we will present a method for the localisation of the exact position of the FBG with a high accuracy. This method is non-invasive and can be utilised at very low complexity, its labour intensity is minimal, and it does not risk the health and the integrity of the optical fibre. The most common alternative to this approach is using a rolling pin over the FBG length, and observe the changes in the reflection spectrum, marking the starting point and ending point of observing changes in the reflection spectrum. However, this method is labour intensive, and its accuracy could be low, since for approximately the first 1 mm of the sensor length, the changes in the reflection spectrum are negligible, and might be confused with different noise sources. Our method is based on mechanically exciting two arbitrary points along the FBG length, and analysing the side-lobes of the FBG reflection spectrum under that momentary stress. For this purpose, we will use the closed form representation of the reflection spectrum that is derived from the approximated transfer matrix method.[7]

Further author information:
E-mail: {a.rajabzadehdizaji, r.c.hendriks, r.heusdens, r.m.groves}@tudelft.nl

Seventh European Workshop on Optical Fibre Sensors, edited by Kyriacos Kalli, Gilberto Brambilla, Sinead O'Keeffe
Proc. of SPIE Vol. 11199, 111990U · © 2019 SPIE · CCC code: 0277-786X/19/$21 · doi: 10.1117/12.2545756

2. PROBLEM FORMULATION

When an FBG sensor experiences a non-uniform strain field (or grating structures), its reflection spectrum can be calculated using numerical methods such as the transfer matrix model.[2] In such cases, it is assumed that the length L of the FBG sensor is divided into M piece-wise uniform segments, each undergoing a uniform strain field. In,[7] we showed that under non-uniform strain fields, the reflection spectrum R of the FBG sensor can be approximated as

$$R(\alpha) \approx \left| \sum_{i=1}^{M} \kappa_i \Delta z \, \mathrm{sinc}(\alpha - \alpha_i) e^{-j\left((M-2i+1)\alpha + \sum_{k<i} \alpha_k - \sum_{k>i} \alpha_k\right)} \right|^2, \tag{1}$$

in which the κ_i's are the coupling coefficients between the forward and backward electric waves, and α and α_i are given by

$$\alpha = \frac{2\pi n_{\text{eff}} \Delta z}{\lambda} \quad \text{and} \quad \alpha_i = \frac{2\pi n_{\text{eff}} \Delta z}{\lambda_i}, \tag{2}$$

respectively. Here, λ is the wavelength region under interrogation, λ_i is the local Bragg wavelength of the i'th segment, and n_{eff} is the effective mode index of the core. In our previous work[8] we showed that there is a linear relationship between the active gauge length of the FBG (even under extremely non-uniform stress fields) and the maximum harmonic frequency of (1). We used this to accurately calculate the active gauge length of the FBG sensor. By rearranging the terms in (1), we showed that the complex reflection spectrum can be presented as[7]

$$\begin{aligned} r(\alpha) = &\sum_{i=1}^{M-1} \overbrace{(\xi_i - \xi_{i+1})}^{\zeta_i} e^{-j\left((M-2i)\alpha + \sum_{k\le i} \alpha_k - \sum_{k>i} \alpha_k\right)} \\ &+ \left(\xi_M e^{jM(\alpha-\bar{\alpha})} - \xi_1 e^{-jM(\alpha-\bar{\alpha})}\right), \end{aligned} \tag{3}$$

where

$$\xi_i = \frac{\kappa_i \Delta z}{2j(\alpha - \alpha_i)}. \tag{4}$$

In this paper, we will focus on the $\zeta_i = \xi_i - \xi_{i+1}$ terms given in (3). As shown in,[5] when there is a smooth stress field over the length of the FBG, the values of ζ_i will be negligible, and the first summation term in (3) can be neglected. On the other hand, if there is a drastic change in the stress or grating distribution at a certain segment of the FBG model, the values of ζ_i at that particular segment will not be negligible anymore. In this work, we will exploit this principle in order to determine the position of the FBG sensor. We put stress at arbitrary (controlled) points along the FBG length, which results in large ζ_i values at the excited segments. As seen from (3), large values of ζ_i result in powerful harmonics at the angular frequency $\omega = M - 2i$ in the complex reflection spectrum. The frequency of such an harmonic is thus directly related to the point of excitation. By finding the precise position of the excitations along the FBG length, the exact position of the sensor can be derived as well. Since in most applications only the amplitude of the reflection spectrum is available, we first need to expand (3). For that purpose, suppose there is only one mechanical excitation at segment t of the FBG model (which means large values for ζ_i at $i = t$). We then get

$$\begin{aligned} R(\alpha) = |r(\alpha)|^2 \approx &\sum_{i=1}^{M-1} |\zeta_i|^2 + 2\,\mathrm{Re}[\zeta_t \zeta_M^*] \cos\left((2M-2t)\alpha + \right. \\ &\left. \theta_t - M\bar{\alpha}\right) - 2\,\mathrm{Re}[\zeta_t \zeta_1^*] \cos\left((2t)\alpha - \theta_i - M\bar{\alpha}\right) + R_r + R_s, \end{aligned} \tag{5}$$

where

$$R_s \approx |\xi_1|^2 + |\xi_M|^2 - 2\mathrm{Re}[\xi_1 \xi_M^*] \cos(2M(\alpha - \bar{\alpha})) \tag{6}$$

refers to the reflection spectrum under a smooth strain field, and R_r is the summation of all remaining terms from the expansion (with lower amplitudes than the other terms in (5)).[8] Note that the information regarding the length of the sensor is in R_s, as the oscillating term in R_s is $\cos(2\pi 2M\Delta z n_{\text{eff}}(1/\lambda - 1/\bar{\lambda}))$, which linearly depends on $L = M\Delta z$. In fact,

this term has the highest oscillation frequency among all the harmonics presented in (5), with a value of $f_{\max} = 2Ln_{\text{eff}}$, from which the exact length of the sensor can be retrieved.[8]

As seen from (5), for a single excitation of the FBG at segment t, two new harmonics will emerge in the reflection spectrum with angular frequencies $\omega = 2M - 2t$ and one at $\omega = 2t$. This means that with a single excitation, one cannot determine the exact location of the excitation, as there will be a reflection line of symmetry ambiguity in localising the excitation. In other words, exciting the sensor at segment t results in the same harmonics as exciting it at segment $M - t$.

In order to overcome this ambiguity, we propose exciting the FBG length at two (or more) locations, and at different time instances, wherein the distance between the excitations is fixed and known. Assume the first excitation is applied at an arbitrary segment, and by inspection of the Fourier transform of the reflection spectrum, we see that the newly generated harmonics have angular frequencies at $\omega = 2t$ and $\omega = 2M - 2t$. With this single excitation, we can deduce that the sensor was stressed either at segment t, or at segment $M - t$. Now, another excitation is applied over the sensor at a known distance of l segments from the first excitation. If the second set of new harmonics are at $\omega = 2(t + l)$ and $\omega = 2M - 2(t + l)$, it means that the first excitation was at the t'th segment. Otherwise, if we see new harmonics at $\omega = 2(M - t + l)$ and $\omega = 2(t - l)$, it means that the first excitation was at the $(M - t)$'th segment. The ambiguity of the excitation point is thus resolved. Moreover, the exact length of the sensor can be retrieved using the method presented in,[8] which determines the overall number of segments M in the FBG model. With the knowledge of the accurate length of the sensor, and the exact excitation segment, the precise start and end point of the sensor can be determined.

The accuracy of this method depends on the width of the excitation, and the narrower the width of the excitation (or the finer the FBG segmentation), the more accurate the localisation accuracy. As a practical example, using small diameter Tungsten wires, excitation points with a width of $10\,\mu m$ can be implemented, using which, a localisation accuracy of $10\,\mu m$ can be achieved. Moreover, by increasing the number of measurements, and averaging the results, the accuracy of the method can be further improved.

3. IMPLEMENTATION

There are several ways to induce the aforementioned local excitations along the FBG length. It can be purely mechanical, using piezo-electric actuators,[9] or by locally heating the FBG sensor. In this paper, we chose the latter option, as it is more easily controllable (in terms of the setup itself, and the width of the excitation). The difference between the mechanical and the thermal excitation is that in the thermal option, the thermo-optic effect is much more dominant than the thermal expansion effect. In fact, the contribution of the thermal expansion to the overall local phase shift has been shown to be around 10% of that of the thermo-optic effects.[10] In such a case, the main effect of locally heating the FBG at segment t is that the effective mode index of the core at that particular segment increases, since $\Delta n_{\text{eff}_t} = a\Delta T$, where a is the thermo-optic coefficient. A qualitative assessment (which is sufficient for the current study) suggests that

$$\Delta n_{\text{eff}_t} \uparrow \;\Rightarrow \Delta\alpha_t \uparrow \;\Rightarrow \Delta\xi_t \uparrow \;\Rightarrow \Delta\zeta_t \uparrow . \tag{7}$$

It is noteworthy that by mechanically exciting segment t of the FBG, the same effect as (7) will be induced, except the origin of the change will be from the local expansion of the FBG at segment t or $\Delta\lambda_t$. With that, our suggested setup for determining the precise position of an FBG sensor is shown in Fig. 1.

In this setup, the Kanthal wires had a diameter of $300\,\mu m$, and we passed around 1 A of current through each of them to heat them up for short periods of time, resulting in temperature changes of around $250\,^{\circ}$C. The FBG used in this study was a partially apodized DTG type sensor from FBGS company, with a Bragg wavelength of 1550 nm and a nominal length of 8 mm. The PXIe-4844 interrogation unit has a wavelength accuracy of 4 pm, and a dynamic range of 40 dB. The objective of this experiment is to determine lengths d_1 and d_2, shown in Fig. 1. Also note that by design $d_2 \approx d_1 + 1$ mm. Since the relative location of the two Kanthal wires are already known, the starting point of the sensor, depicted by "ref" in the figure, can be determined.

In order to analyse the reflection spectrum side-lobes given in (5), we apply a Hann window on the reflection spectrum, starting at the centre of mass of the reflection spectrum, given by

$$\lambda_{B_c} = \frac{\int_\lambda \lambda R(\lambda)\mathrm{d}\lambda}{\int_\lambda R(\lambda)\mathrm{d}\lambda}, \tag{8}$$

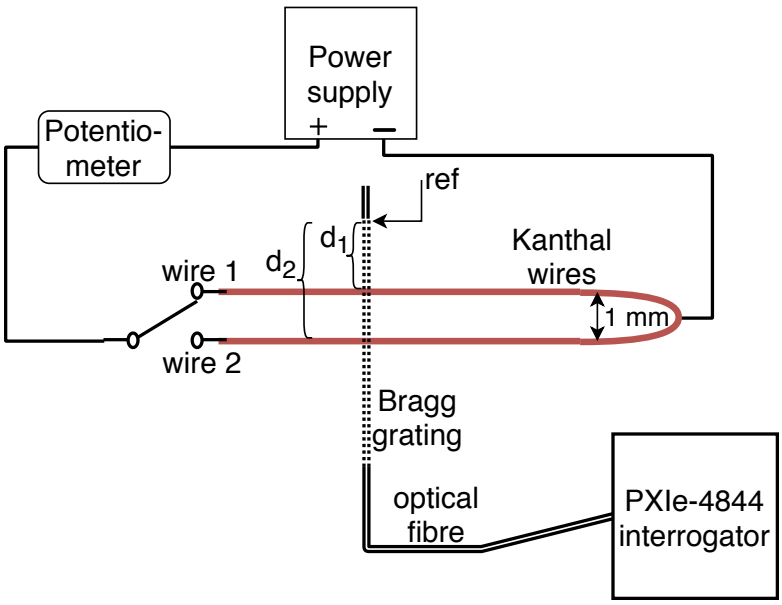

Figure 1: The setup used for determination of the position of the FBG sensor. The manual switch determines which of the two Kanthal wires, denoted by wire 1 and wire 2, will be connected to the power supply. "ref" denotes the starting point of the sensor, and d_1 and d_2 are the distances of wire 1 and wire 2 from the "ref" point, respectively.

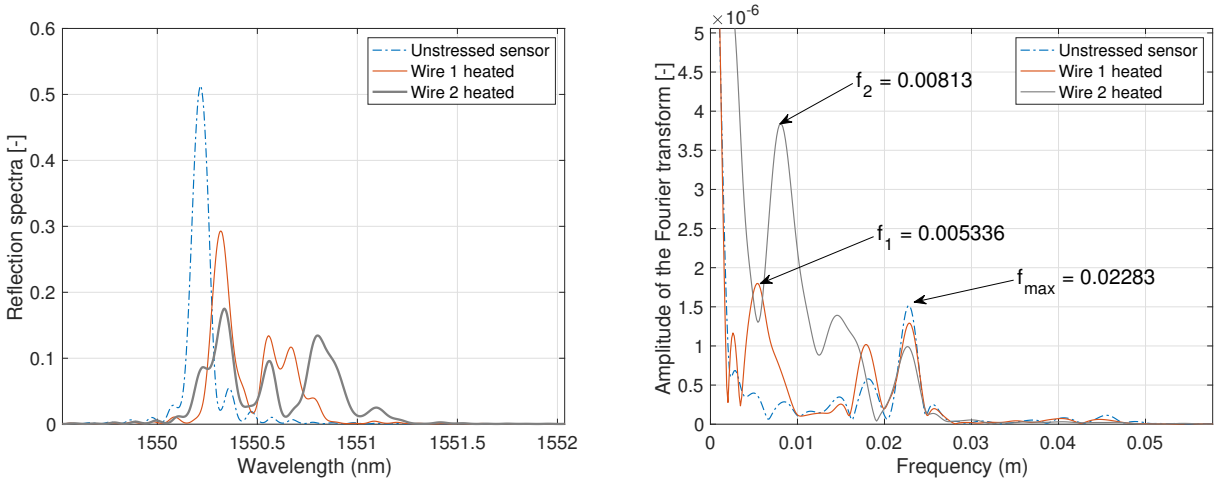

(a) (b)

Figure 2: (a): Reflection spectrum from a healthy FBG, along with the reflection spectra of the same sensor when wire 1 and wire 2 were heated. (b): The associated Fourier transform of the windowed side-lobes.

where λ is the wavelength region under investigation. The upper bound was chosen by setting a threshold on the amplitude of the reflection spectrum, and truncating the spectrum outside this interval. Fig. 2a shows the reflection spectra of the sample DTG sensor in Fig. 1, in three different time instances associated with the unstressed sensor, and with heating of the two Kanthal wires. Applying the Hann window on the reflection spectrum, and taking the Fourier transform of the side-lobes results in the graphs of Fig. 2b. Note that in Fig. 2b, the 'x' axis is scaled by a factor of Δz, and thus, the retrieved distances will be in 'mm' rather than segment numbers.

It can be seen from Fig. 2b that the retrieved length of the sensor in this example is $L = f_{\max}/(2n_{\text{eff}}) = 7.8892$ mm.[8] In the first instance of locally heating the FBG via wire 1, the emerging harmonics are at $f_1 = 0.005336$ m and $f_1' = 0.0177$ m. Note the symmetry of the location of the new harmonics with respect to the central frequency in the Fourier domain at $f_c = f_{\max}/2 = 0.0114$ m. From this first measurement, it can be deducted that wire 1 is either at

$d_1 = f_1/(2n_{\text{eff}}) = 1.8439$ mm or at $d_1' = f_1'/(2n_{\text{eff}}) = 6.1165$ mm distance from the reference point "ref". By inspection of the FBG reflection spectrum when locally heated via wire 2, the retrieved distance of wire 2 from the reference point is either $d_2 = f_2/(2n_{\text{eff}}) = 2.8094$ mm or $d_2' = f_2'/(2n_{\text{eff}}) = 5.0901$ mm. Based on these two measurements, and taking into account the fact that $d_2 \approx d_1 + 1$ mm, it can be concluded that $d_1 = 1.8439$ mm and $d_2 = 2.8094$ mm, and the precise location of the "ref" point (start point of the sensor) is determined to be at a distance of d_1 from wire 1.

4. CONCLUSIONS AND DISCUSSIONS

In this study, we showed that using two sets of measurements in a controlled setup of locally exciting arbitrary points of an FBG sensor, the precise position of the FBG can be retrieved. Such accurate information is beneficial in damage detection type applications of FBG sensors, to provide information about the location of the damage (matrix cracks of delamination tip) with a high spatial resolution. Our method can also be used for accurate marking of the sensor position on optical fibres during their production as well. Furthermore, by altering the setup to simultaneous excitations of the two Kanthal wires at different distances from each other, our method can work for fully apodized FBG sensors as well.

Acknowledgement

This research is part of the TKI Smart Sensing for Aviation Project, sponsored by the Dutch Ministry of Economic Affairs under the Topsectoren policy for High Tech Systems and Materials, and industry partners Airbus Defence and Space, Fokker Technologies — GKN Aerospace and Royal Schiphol Group.

REFERENCES

[1] E. Udd, W. B. Spillman Jr, "Fiber Optic Sensors: An Introduction for Engineers and Scientists," John Wiley & Sons (2011).

[2] T. Erdogan, "Fiber grating spectra," J. Lightw. Technol., **15(8)**, 1277-1294 (1997).

[3] Y. Okabe, T. Mizutani, S. Yashiro, N. Takeda, "Detection of microscopic damages in composite laminates," Composites science and technology, 62(**7-8**), 951-958, 2002.

[4] S. Takeda, Y. Okabe, N. Takeda, "Monitoring of delamination growth in CFRP laminates using chirped FBG sensors," Journal of Intelligent Material Systems and Structures, 19(**4**), 437-444, 2008.

[5] A. Rajabzadeh, R. Heusdens, R. C. Hendriks, R. M. Groves, "Characterisation of Transverse Matrix Cracks in Composite Materials Using Fibre Bragg Grating Sensors," J. Lightw. Technol., 2019.

[6] A. D. Kersey, M. A. Davis, H. J. Patrick, M. LeBlanc, K. P. Koo, C. G. Askins, M. A. Putnam, and E. J. Friebele, "Fiber grating sensors," J. Lightw. Technol., **15**, 1442-1463 (1997).

[7] A. Rajabzadeh, R. Heusdens, R. C. Hendriks, and R. M. Groves, "Calculation of the mean strain of smooth non-uniform strain fields using conventional FBG sensors," J. Lightw. Technol., **36(17)**, 3716-3725 (2018).

[8] A. Rajabzadeh, R. Heusdens, R. C. Hendriks, R. Groves, "A Method for Determining the Length of FBG Sensors Accurately," IEEE Photonics Technology Letters, **31(2)**, 197-200 (2019).

[9] J. Palaci, P. Perez-Millan, G. E. Villanueva, J. L. Cruz, M. V. Andres, J. Marti, B. Vidal, "Tunable photonic microwave filter with single bandpass based on a phase-shifted fiber Bragg grating," IEEE Photonics Technology Letters, 22(**19**) 1467-1469 (2010).

[10] Z. Zhang, C. Tian, M. R. Mokhtar, P. Petropoulos, D. J. Richardson, M. Ibsen, "Rapidly reconfigurable optical phase encoder-decoders based on fiber Bragg gratings," IEEE photonics technology letters, **18(11)**, 1216-1218 (2006).